

A novel method to recover DD fusion proton CR-39 data corrupted by fast ablator ions at OMEGA and the National Ignition Facility

G. D. Sutcliffe, L. M. Milanese, D. Orozco, B. Lahmann, M. Gatu Johnson, F. H. Séguin, H. Sio, J. A. Frenje, C. K. Li, R. D. Petrasso, H.-S. Park, J. R. Rygg, D. T. Casey, R. Bionta, D. P. Turnbull, C. M. Huntington, J. S. Ross, A. B. Zylstra, M. J. Rosenberg, and V. Yu. Glebov

Citation: *Review of Scientific Instruments* **87**, 11D812 (2016); doi: 10.1063/1.4960072

View online: <http://dx.doi.org/10.1063/1.4960072>

View Table of Contents: <http://scitation.aip.org/content/aip/journal/rsi/87/11?ver=pdfcov>

Published by the [AIP Publishing](#)

Articles you may be interested in

[Proton pinhole imaging on the National Ignition Facility](#)

Rev. Sci. Instrum. **87**, 11E704 (2016); 10.1063/1.4959782

[A method for in situ absolute DD yield calibration of neutron time-of-flight detectors on OMEGA using CR-39-based proton detectors](#)

Rev. Sci. Instrum. **86**, 053506 (2015); 10.1063/1.4919290

[A technique for extending by ~103 the dynamic range of compact proton spectrometers for diagnosing ICF implosions on the National Ignition Facility and OMEGAa\)](#)

Rev. Sci. Instrum. **85**, 11E119 (2014); 10.1063/1.4892439

[Prototypes of National Ignition Facility neutron time-of-flight detectors tested on OMEGA](#)

Rev. Sci. Instrum. **75**, 3559 (2004); 10.1063/1.1788875

[Absolute measurements of neutron yields from DD and DT implosions at the OMEGA laser facility using CR-39 track detectors](#)

Rev. Sci. Instrum. **73**, 2597 (2002); 10.1063/1.1487889

**PHYSICS
TODAY**

Welcome to a

Smarter Search 

with the redesigned
Physics Today Buyer's Guide

Find the tools you're looking for today!

A novel method to recover DD fusion proton CR-39 data corrupted by fast ablator ions at OMEGA and the National Ignition Facility

G. D. Sutcliffe,^{1,a)} L. M. Milanese,¹ D. Orozco,¹ B. Lahmann,¹ M. Gatu Johnson,¹ F. H. Séguin,¹ H. Sio,¹ J. A. Frenje,¹ C. K. Li,¹ R. D. Petrasso,¹ H.-S. Park,² J. R. Rygg,² D. T. Casey,² R. Bionta,² D. P. Turnbull,² C. M. Huntington,² J. S. Ross,² A. B. Zylstra,³ M. J. Rosenberg,⁴ and V. Yu. Glebov⁴

¹Plasma Science and Fusion Center, Massachusetts Institute of Technology, Cambridge, Massachusetts 02139, USA

²Lawrence Livermore National Laboratory, Livermore, California 94550, USA

³Los Alamos National Laboratory, Los Alamos, New Mexico 87545, USA

⁴Laboratory for Laser Energetics, Rochester, New York 14623, USA

(Presented 7 June 2016; received 6 June 2016; accepted 8 July 2016; published online 5 August 2016)

CR-39 detectors are used routinely in inertial confinement fusion (ICF) experiments as a part of nuclear diagnostics. CR-39 is filtered to stop fast ablator ions which have been accelerated from an ICF implosion due to electric fields caused by laser-plasma interactions. In some experiments, the filtering is insufficient to block these ions and the fusion-product signal tracks are lost in the large background of accelerated ion tracks. A technique for recovering signal in these scenarios has been developed, tested, and implemented successfully. The technique involves removing material from the surface of the CR-39 to a depth beyond the endpoint of the ablator ion tracks. The technique preserves signal magnitude (yield) as well as structure in radiograph images. The technique is effective when signal particle range is at least 10 μm deeper than the necessary bulk material removal. *Published by AIP Publishing.* [<http://dx.doi.org/10.1063/1.4960072>]

I. INTRODUCTION

CR-39 is a plastic particle track detector. High energy density (HED) and inertial confinement fusion (ICF) facilities use CR-39 in a variety of nuclear diagnostics, including particle spectrometers and proton radiography.^{1,2} All of these diagnostics employ some degree of filtering in front of the CR-39 to stop background ions from impinging on the detector, and to range high-energy nuclear products down to the appropriate energies for efficient detection. CR-39 has a detection efficiency of 100% for protons in the 500-keV to 6-MeV energy range and is essentially insensitive to electromagnetic radiation, which makes it a powerful detector for ICF and HED applications.³ High laser intensities drive plasma instabilities and acceleration of fast ions.^{4,5} Much effort has been devoted to the study of the empirical conditions which drive these instabilities and how maximum ion energy scales with laser intensity.^{6–8} On-target laser intensities approaching 10^{15} W/cm² in OMEGA ICF implosions result in fast ablator ion energy endpoints of order ~ 1 MeV.⁹ Certain HED plasma experiments at OMEGA and the National Ignition Facility (NIF) have configurations with unique geometries and unusually high laser intensity which result in large fast ablator ion energies. The most penetrating of these ions are typically protons, even

when target material is not nominally hydrogenous—trace surface contamination with water or hydrocarbons is a source of protons.^{7,10}

For detection of the 3.02-MeV protons from the D(d,t)p reaction (referred to in this paper as “DD-protons”), thin (~ 15 μm Ta or equivalent) filtering is used. Because of this, fast ablator ions accelerated from the implosion or HED plasma sometimes penetrate the filtering and impinge on the CR-39. This effect is not an issue for measurements of the 14.7-MeV protons from the He-3(d, α)p reaction (here referred to as “D³He-protons”) because thick filtering (~ 1000 μm Al) is used to reduce the energy for CR-39 detection. The fast ablator ions are generated with much higher fluences (roughly $\sim 10^{14}$ protons above 500 keV in Ref. 9) than the DD-protons (10^{10} for D³He-proton backlighters at the NIF¹¹), and thus obscure the signal once the tracks are developed through track etching. In recent experiments, CR-39 data have been corrupted by this effect—see Fig. 1.

Depending on the available instrumentation, the endpoint energy of the spectrum of the fast ablator ions can be constrained. In the case of charged particle spectrometers (CPSs)² on OMEGA, the endpoint can be accurately determined. If step-range-filter (SRF) instruments¹² are used, the endpoint can often be constrained by the thickness of the first filter through which the fast ablator ions did not penetrate.

This paper will be organized as follows: Sec. II describes the data recovery method, Sec. III outlines the testing and validation of this method, and Sec. IV discusses the successful application to real data.

Note: Contributed paper, published as part of the Proceedings of the 21st Topical Conference on High-Temperature Plasma Diagnostics, Madison, Wisconsin, USA, June 2016.

^{a)}Author to whom correspondence should be addressed. Electronic mail: gdsut@mit.edu.

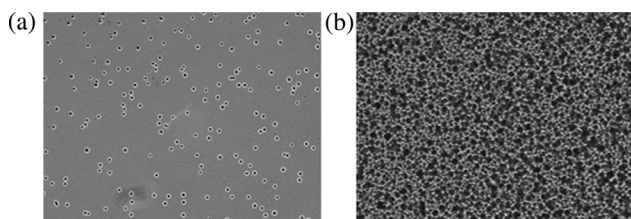


FIG. 1. (a) A microscope image of ideal CR-39 proton data¹¹—tracks are large, high contrast, and do not overlap each other. (b) A microscope image of CR-39 corrupted by a large fluence of fast ablator ions accelerated from an implosion—these tracks totally overwhelm and obscure the underlying signal.¹¹ Image dimensions are approximately $400\ \mu\text{m} \times 300\ \mu\text{m}$.

II. DATA RECOVERY PROCEDURE

A method has been developed for the recovery of the DD-proton data from fast ablator ion corruption. This procedure relies on the range of the signal particles in CR-39 being longer than that of the fast ablator ions. CR-39 material that has been corrupted with the ablator ions is first removed, then the process for track development is performed to develop the remaining tracks. If the endpoint energy of the fast ablator ions is known, the depth of the bulk-etch removal can be chosen beyond the depth of the affected CR-39. If it is not known, the depth can be chosen from prior knowledge of fast ablator ions from similar shots and the process is repeated if the fast ablator ion tracks reappear. This technique leverages the “bulk-etch” procedure (an etch where the bulk removal rate is roughly equal to the track etch rate^{8,13,14}) for removing CR-39 material and erasing the tracks from the original “track-etch” (an etch which preferentially develops particle tracks), and is used in applications like track coincidence counting.¹³ The track etch itself has an associated bulk removal rate, roughly $2.6\ \mu\text{m}/\text{h}$.¹⁵ The application discussed in this paper uses smaller depth removals ($\sim 20\ \mu\text{m}$) with higher etching accuracy ($\sim 10\ \mu\text{m}$) than the coincidence counting technique.

III. TESTING AND VALIDATION

Tests of this method were carried out on a wide range of data: a mock-up experiment was conducted at MIT HED’s accelerator facility before its application to important data obtained at OMEGA and the NIF.

A. Testing the method—Accelerator facility

The MIT-HED LEIA (linear electrostatic ion accelerator) facility¹⁶ was used to test the effects of high-fluence particle background on signal track data. A 135-keV deuterium beam was incident on an ErD_2 -target doped with ^3He to create DD and D^3He fusion products. CR-39 detectors were fielded with a step-filter arrangement (no filtering, $3\ \mu\text{m}$ Mylar, $20\ \mu\text{m}$ Al, $50\ \mu\text{m}$ Al). Scattered beam deuterons were used as surrogate high-fluence fast ablator ions in the region of the detector which had no filtering. The different filter thicknesses allowed for the investigation of bulk-etch depth accuracy. The signals present in this study are the tracks from 3.02-MeV protons and 1.01-MeV tritons from $\text{D}(\text{d,t})\text{p}$ reactions, as well

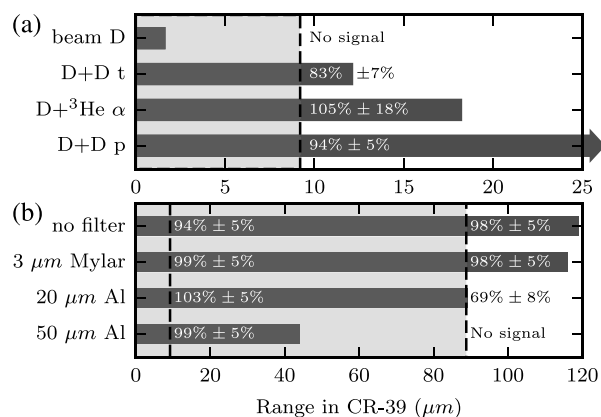


FIG. 2. Summary of accelerator data recovery experiments. The range (solid bars) of particles, bulk etch depths (dotted lines, shaded), and signal recovery rates corresponding to bulk etch depths are shown. (a) shows predicted particle ranges and bulk material removed in the no-filter region; (b) shows 3.02-MeV DD-proton depths in all four filtering regions, as well as the two relevant bulk etch depths. The ranges of the particles have associated variations from straggling, which are not shown. Uncertainties from recovery are dominated by how well particle signals can be distinguished—larger errors are assigned when signal peaks in diameter-contrast (track characteristics) space are hard to distinguish.

as those from the 3.6-MeV α from ^3He ($\text{d,p})\alpha$ reactions. The 0.82-MeV ^3He signal from the $\text{D}(\text{d,n})^3\text{He}$ reaction is below the threshold for detection when filtering is used and is therefore not considered. Particle penetration depths are calculated using SRIM.¹⁷ The experiment is summarized in Fig. 2. Nominal bulk-etch depths listed are those as measured during the procedure; however, a number of procedural factors contribute to uncertainty in this number—the goal here is thus to understand how close the nominal bulk-etch can come to the signal particle mean range without losing signal.

Using a short bulk etch ($4\ \mu\text{m}$ nominal bulk etch + $5.2\ \mu\text{m}$ from track etch) designed to recover all three types of particle signals of interest, proton and α counts matched expected yields within uncertainty. Tritium signal (at $12.1\ \mu\text{m}$ depth $\pm 0.5\ \mu\text{m}$ straggling) was partially lost ($83\% \pm 7\%$ of the expected signal), indicating that uncertainties in the bulk-etch process exceeded the available $\sim 3\ \mu\text{m}$ margin (signal particle mean range less total bulk nominal removal depth). The full recovery of the 3.6-MeV α signal (at $18.2\ \mu\text{m}$ depth $\pm 0.6\ \mu\text{m}$ straggling) with $\sim 9\ \mu\text{m}$ margin was the smallest margin for which signal was fully recovered. Using a long bulk-etch ($83.6\ \mu\text{m}$ nominal bulk etch + $5.2\ \mu\text{m}$ from track etch), proton signals were accurately recovered in the regions with thin Mylar or no filtering; however, the proton signal was affected ($69\% \pm 8\%$ of expected signal) in the $20\ \mu\text{m}$ Al filtering region, where the proton range was $89\ \mu\text{m}$ depth $\pm 5\ \mu\text{m}$ straggling (nominally, the bulk etch depth was within $\sim 1\ \mu\text{m}$ of the mean signal particle range). This supports the bulk-etch accuracy limit found in the tritium-signal case above, and puts a realistic lower bound on penetration depth separation between signal and background tracks required to accurately recover the signal. Additionally, controlling long bulk etches to $< 5\ \mu\text{m}$ precision is challenging due to the variability of the bulk-etch rate—the target bulk etch depth in this case was $80\ \mu\text{m}$.

As seen from the recovery of the 3.6-MeV α signal in the shallow bulk etch case, the signal particle tracks should be at least $10\ \mu\text{m}$ deeper than the range of background tracks for full data recovery—this was the smallest margin for which data were successfully recovered.

B. Testing the effect of the method on radiography image quality

Proton radiography is used to image electric and magnetic fields in the interacting regions of plasmas.¹ A backlighter capsule with D^3He fuel is imploded to generate 3.02-MeV and 14.7-MeV protons, which are deflected by fields in an interacting region en route to a stack of two 10-cm square 1.5-mm thick CR-39 detectors; the front CR-39 is typically filtered by a $12.5\text{-}\mu\text{m}$ Ta foil. The front CR-39 is sensitive to the DD-protons, while the back CR-39 is sensitive to the D^3He -protons. Radiography images show the density of protons from the backlighter; structure in these images is critical for data interpretation.¹ To test the image quality fidelity of the method, an unaffected proton radiography piece with well-defined, high contrast structures was processed and analyzed using the recovery method: a $20\text{-}\mu\text{m}$ bulk-etch was performed, followed by a 1-h track-etch (total material removed, including original 1-h track-etch: $\sim 25\ \mu\text{m}$). The images before and after, seen in Fig. 3, are nearly indistinguishable, showing that the procedure has no effect on image quality. A comparison of the radiographs in Fig. 3 shows that image imperfections due to (track-similar) surface defects in the CR-39 have been removed. This reveals an extension of the capabilities of this method: the removal of CR-39 surface defects.

IV. RECOVERY OF DATA FROM OMEGA AND THE NIF

The DD-proton data recovery method was applied to various affected OMEGA and NIF data sets.

A. Recovery of DD-proton data obtained at the NIF

A CR-39-based SRF¹⁰ was fielded on the NIF for measurements of DD-proton yield.¹¹ The filtering was in $5\text{-}\mu\text{m}$ Ta steps ranging from $5\ \mu\text{m}$ to $20\ \mu\text{m}$, and the fast ablator ions only penetrated the thinnest filter (see Fig. 4), which sets an upper

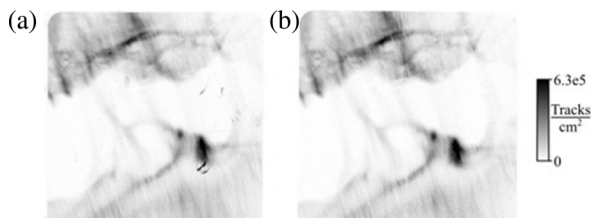


FIG. 3. Demonstration that recovery method does not affect image quality. Comparison of 10-cm square radiographic images (a) before and (b) after the data recovery method was applied to a piece of data unaffected by fast ablator ions. Dark sharp structures on (a) which do not appear on (b) are from surface defects in the CR-39. Track density scales are the same between both images, with darker indicating a higher density of tracks. Data come from OMEGA shot 76487 on 2015/03/10.

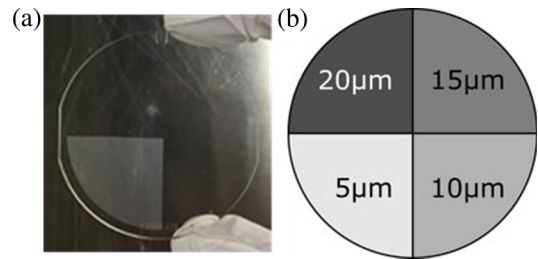


FIG. 4. NIF SRF fast ablator ion corruption: (a) visible clouding from fast ablator ions behind the $5\text{-}\mu\text{m}$ Ta filter; (b) Ta filter configuration on NIF shot N150326-001.¹¹ Detector is 5 cm in diameter.

limit on the energy endpoint of the ions: $E_{\text{max}} \leq 1.31\ \text{MeV}$, with a corresponding maximum penetration depth in CR-39 after the $5\text{-}\mu\text{m}$ Ta filter of $13.1\ \mu\text{m} \pm 0.6\ \mu\text{m}$ (here the ions are assumed to be protons because protons penetrate deeper than higher- Z particles, and thus represent an upper bound on the range in CR-39). The bulk-etch depth was chosen to exceed this depth. The other regions with different filter thicknesses provide a baseline for expected particle counts—these should be unaffected after the process is applied. Fig. 5 shows the successful recovery of the DD-proton signal in the affected region. The signal here matched those from the unaffected regions within uncertainty. The signals in the unaffected regions before and after the procedure agreed considering the uncertainty.

B. Recovery of OMEGA proton radiography data

In some circumstances, fast ablator ions are energetic enough to penetrate the filtering on CR-39 proton radiography diagnostics and obscure the DD-proton data. In experiments at OMEGA exploring astrophysical collisionless shocks,¹⁸ fast ablator ions penetrated the $12.5\text{-}\mu\text{m}$ Ta filtering and obscured the DD-proton data on the front CR-39. The original track-etch, which revealed the ablator ion tracks, took 1.5 h. Using the data-recovery technique, the DD-proton data could be recovered (see Fig. 6).

In this instance, a $20\text{-}\mu\text{m}$ bulk-etch was performed, followed by a 1-h track-etch (total material removed, including original track-etch: $\sim 27\ \mu\text{m}$). Bulk etch depth choice was motivated by previous experience and proton penetration depth calculations in SRIM.¹⁷ The measured DD-proton yield matched the measured DD-neutron yields within 25% (these

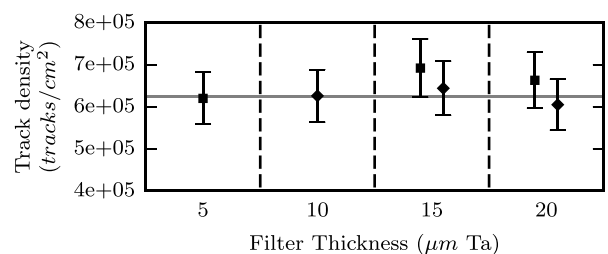


FIG. 5. Recovery method does not affect measured yields. Track densities in each region, showing signals before (diamonds) and after (squares) applying the recovery method. The solid horizontal line shows the mean track density ($6.25 \times 10^5\ \text{tracks/cm}^2$) in the unaffected regions before the procedure. The data in the $10\text{-}\mu\text{m}$ region after the bulk-etch were not recorded.

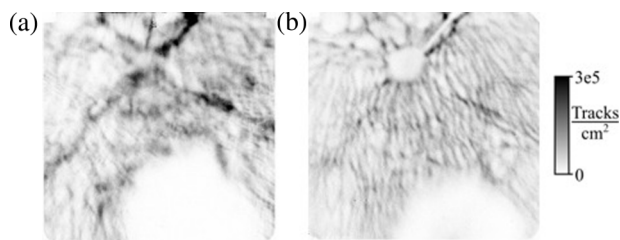


FIG. 6. (a) Recovered 10-cm square DD-proton radiograph; (b) corresponding $D^3\text{He}$ -proton radiograph (not affected by fast ablator ions), showing similar structures. Data come from OMEGA shot 76497 on 2015/03/10. In this instance, a “before” radiograph is unavailable, but track counts are at least 10 times higher than in the above radiographs.

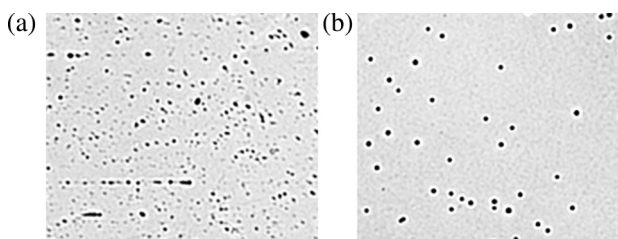


FIG. 7. Excerpts of microscope images of tracks on CR-39 (a) before and (b) after the recovery method was applied. Signal tracks are DD-protons, while background tracks in 7a are ablator ions. Data are from NIF shot N160329-005. Frame dimensions are $130\ \mu\text{m} \times 115\ \mu\text{m}$.

are not expected to be identical because deflection of protons by fields in the experimental region away from the detector would reduce the measured fluence). Large-scale structures (target stalk, laser spots) in the recovered DD radiograph are qualitatively similar to those in the $D^3\text{He}$ -proton radiograph. Small fluctuations observed in the images were not expected to match because DD-protons probe the experiment volumes at a different time than the $D^3\text{He}$ -protons and are deflected differently. This, in conjunction with the study to test variation of spatial structures as a result of the procedure, leads to the conclusion that the radiograph had been successfully recovered.

C. Recovery of NIF proton radiography data

Proton radiography data from a March 2016 NIF shot investigating astrophysical collisionless shocks was affected by fast ablator ion corruption. The filtering in this case was $25\ \mu\text{m}$ Zr, which corresponds to fast ablator ion energies (assuming protons) of at least 1.85-MeV. The source of the ablator ions is uncertain.¹⁹ The recovery method was applied (bulk etch $\sim 25\ \mu\text{m}$, total material removed $\sim 33\ \mu\text{m}$ including track-etches before and after); representative microscope images of the tracks can be seen in Fig. 7.

Fig. 7(a) shows the presence of extra tracks that are hard to distinguish from signal tracks. The method successfully eliminated the background tracks while keeping the signal tracks, shown in Fig. 7(b).

V. CONCLUSION

A novel method has been developed to recover low-energy nuclear signal data (DD-protons, DD-tritons, $D^3\text{He}$ -alphas) in the presence of high-fluence ablator ions. The minimum depth separation between the signal depth (less straggling) and total nominal bulk-etch depth (includes material removed in track etch) for full signal recovery is approximately $10\ \mu\text{m}$. This study also addressed concerns about the fidelity of this technique with regard to both yield and image data—image quality was preserved through the process. While filtering can be designed based on anticipated fast ablator ion energies, unexpected upshifts in ion energies or downshifts in signal proton energies forces filter design to be conservative. There will therefore always be some chance of fast ablator ions penetrating the filtering. Knowledge of the spectrum of the fast ablator ions (or at least the maximum energy) aids greatly in applying this method, because the maximum range of the fast ablator ions can be determined. This technique is useful as a back-up tool for data recovery in the situations where data are obscured by fast ablator ions. This technique has been routinely applied to recovering data from experiments at both OMEGA and the NIF.

ACKNOWLEDGMENTS

The authors thank R. Frankel and E. Doeg for contributing to the CR-39 processing. This work was supported in part by the U.S. DoE (No. DE_NA0002949), NLUF (No. DE_NA0002726), LLNL (No. 613027), LLE (No. 416107-G), and LANL (No. 334926).

- ¹C. K. Li *et al.*, *Rev. Sci. Instrum.* **77**, 10E725 (2006).
- ²D. G. Hicks *et al.*, *Rev. Sci. Instrum.* **68**, 589 (1997).
- ³F. H. Séguin *et al.*, *Rev. Sci. Instrum.* **74**, 975 (2003).
- ⁴A. B. Zylstra *et al.*, *Phys. Plasmas* **19**, 042707 (2012).
- ⁵Y. Kishimoto, K. Mima, T. Watanabe, and K. Nishikawa, *Phys. Fluids* **26**, 2308 (1983).
- ⁶T. Tan, G. McCall, and A. Williams, *Phys. Fluids* **27**, 296 (1984).
- ⁷S. J. Gitomer, R. D. Jones, F. Begay, A. W. Ehler, J. F. Kephart, and R. Kristal, *Phys. Fluids* **29**, 2679 (1986).
- ⁸P. Wägli, T. P. Donaldson, and P. Lädach, *Appl. Phys. Lett.* **32**, 638 (1978).
- ⁹D. G. Hicks *et al.*, *Phys. Plasmas* **8**, 606 (2001).
- ¹⁰N. Sinenian *et al.*, *Appl. Phys. Lett.* **101**, 114102 (2012).
- ¹¹J. R. Rygg *et al.*, *Rev. Sci. Instrum.* **86**, 116104 (2015).
- ¹²M. J. Rosenberg *et al.*, *Rev. Sci. Instrum.* **85**, 103504 (2014).
- ¹³D. T. Casey *et al.*, *Rev. Sci. Instrum.* **82**, 073502 (2011).
- ¹⁴S. A. Amin and D. L. Henshaw, *Nucl. Instrum. Methods Phys. Res.* **190**, 2 (1981).
- ¹⁵J. Rojas-Herrera *et al.*, *Rev. Sci. Instrum.* **86**, 033501 (2015).
- ¹⁶N. Sinenian *et al.*, *Rev. Sci. Instrum.* **83**, 043502 (2012).
- ¹⁷J. F. Ziegler, M. D. Ziegler, and J. P. Biersack, *Nucl. Instrum. Methods Phys. Res.* **268**, 1818 (2010).
- ¹⁸C. M. Huntington *et al.*, *Nat. Phys.* **11**, 173 (2015).
- ¹⁹Previous experiments, identical except without a backlighter using thinner radiography filtering ($12.5\ \mu\text{m}$ Ta), saw no ablator ion tracks. The backlighter in this shot (N160329) was similar to that in Figure 4 (N150326), where $10\ \mu\text{m}$ Ta filtering was sufficient to filter out the ablators—the difference in N160329 was that the backlighter illumination was highly asymmetric. The increased intensities and overlap of beams on the backlighter could be the cause of the higher ablator ion energies.